Carbohydrate Polymers 98 (2013) 877–885

Contents lists available at SciVerse ScienceDirect

Carbohydrate Polymers

journal homepage: www.elsevier.com/locate/carbpol

Pectin/carboxymethyl cellulose/microfibrillated cellulose composite scaffolds for tissue engineering

Neethu Ninan[a,c,*], Muthunarayanan Muthiah[b], In-Kyu Park[b], Anne Elain[a], Sabu Thomas[c], Yves Grohens[a]

[a] Université de Bretagne Sud, Laboratoire Ingénierie des Matériaux de Bretagne, BP 92116, 56321 Lorient Cedex, France
[b] Department of Biomedical Sciences and Center for Biomedical Human Resources (BK-21 project), Chonnam National University Medical School, Gwangju 501-757, South Korea
[c] Centre for Nanoscience and Nanotechnology and School of Chemical Sciences, Mahatma Gandhi University, Priyadarsini Hills PO, Kottayam 686560, Kerala, India

ARTICLE INFO

Article history:
Received 6 March 2013
Received in revised form 18 June 2013
Accepted 28 June 2013
Available online 7 July 2013

Keywords:
Pectin
Carboxymethyl cellulose
Microfibrillated cellulose
Lyophilisation
Scaffold
Porosity

ABSTRACT

Highly porous three-dimensional scaffolds made of biopolymers are of great interest in tissue engineering applications. A novel scaffold composed of pectin, carboxymethyl cellulose (CMC) and microfibrillated cellulose (MFC) were synthesised using lyophilisation technique. The optimised scaffold with 0.1% MFC, C(0.1%), showed highest compression modulus (~3.987 MPa) and glass transition temperature (~103 °C). The pore size for the control scaffold, C(0%), was in the range of 30–300 μm while it was significantly reduced to 10–250 μm in case of C(0.1%). Using micro computed tomography, the porosity of C(0.1%) was estimated to be 88%. C(0.1%) showed excellent thermal stability and lower degradation rate compared to C(0%). The prepared samples were also characterised using XRD and FTIR. C(0.1%) showed controlled water uptake ability and *in vitro* degradation in PBS. It exhibited highest cell viability on NIH3T3 fibroblast cell line. These results suggest that these biocompatible composite scaffolds can be used for tissue engineering applications.

1. Introduction

Biopolymers are of immense interest in tissue engineering as they are cytofriendly, biodegradable and contain bio-functional molecules that aid in the attachment, proliferation and differentiation of cells (Van Vlierberghe, Dubruel, & Schacht, 2011). Polysaccharides are ubiquitous biopolymers consisting of monosaccharides, joined together by glycosidic bonds (García-González, Alnaief, & Smirnova, 2011). They have several advantages including low toxicity, good biocompatibility, low cost and chemical resemblance to bioactive glycosaminoglycan molecules in the extracellular matrix of mammalian tissues (Malafaya, Silva, & Reis, 2007). Various naturally occurring polysaccharides are used for fabrication of tissue engineering scaffolds including starch (Rodrigues, Gomes, Leonor, & Reis, 2012), alginate (Shachar, Tsur-Gang, Dvir, Leor, & Cohen, 2011), chitin (Sudheesh Kumar et al., 2011), chitosan (Sionkowska & Płanecka, 2013), hyaluronic acid (Lee & Kurisawa, 2013), cellulose (Pooyan, Tannenbaum, & Garmestani, 2012), pectin (Coimbra et al., 2011) and agarose (Khanarian, Haney, Burga, & Lu, 2012). Pectin is a heterosaccharide found in terrestrial plant cell wall, consisting mainly of esterified D-galacturonic acid residues in α-(1→4) chains (Nunes et al., 2012). It is a polyuronate which on subjected to calcium induced gelation results in the formation of egg box like structures that enable immobilisation of bioactive components or cells inside the gel structure (Munarin et al., 2011). Pectin based biomaterials are used for tissue engineering (Coimbra et al., 2011), wound dressing (Munarin, Tanzi, & Petrini, 2012), gene transfer (Katav et al., 2008), drug delivery (Smistad, Bøyum, Alund, Samuelsen, & Hiorth, 2012) and cancer targeting (Dutta & Sahu, 2012). However, due to poor mechanical properties, it is mostly blended with other polymers.

Carboxymethyl cellulose (CMC) is a water soluble derivative of cellulose with β-(1→4) glucopyranose residues and has adverse uses in dermal tissue engineering (Ramli & Wong, 2011), pulp cell regeneration (Chen & Fan, 2007), protein delivery (Tripathy & Raichur, 2013) and prevention of post-surgical adhesions (Di Spiezio Sardo et al., 2011). Due to its polyelectrolyte nature, it is used as an excellent superabsorbent (Wang & Wang, 2010). It also acts as a viscosity modifier, thickener and emulsifier

* Corresponding author at: Laboratoire d'Ingénierie des MATériaux de Bretagne (LIMatB), Centre de Recherche Christiaan Huygens, Rue de St Maudé – BP 92116, Bureau 32 bis, Université de Bretagne-Sud, 56321 Lorient Cedex, France.
Tel.: +33 751464109/+91 0484 2557031; fax: +33 0 2 97 87 45 19.
E-mail address: neethuninan85@yahoo.co.in (N. Ninan).

0144-8617/$ – see front matter © 2013 Elsevier Ltd. All rights reserved.
http://dx.doi.org/10.1016/j.carbpol.2013.06.067

(Ghanbarzadeh & Almasi, 2011). Microfibrillated cellulose (MFC) is composed of expanded high volume cellulose obtained by mechanical disintegration of cellulosic material without the use of hydrolysis. MFC constitutes aggregates of long cellulose microfibrils of diameter ranging from 20 to 60 nm. It contains amorphous as well as crystalline parts and forms a web like structure. It has low percolation threshold and has a very good ability to form stable network (Lavoine, Desloges, Dufresne, & Bras, 2012). It has gained a lot of importance as filler material in the manufacture of biocomposites made of polymers like polyvinyl alcohol (Qiu & Netravali, 2012), poly lactic acid (Suryanegara, Nakagaito, & Yano, 2009), polycaprolactone (Lönnberg, Fogelström, Berglund, Malmström, & Hult, 2008), pectin (Agoda-Tandjawa, Durand, Gaillard, Garnier, & Doublier, 2012), starch (Wan et al., 2009), *etc.*

There are different methods to synthesise porous biocomposite scaffolds like solvent casting/particulate leaching (Sin et al., 2010), thermally induced phase separation (Shao, Chen, Wang, Chen, & Du, 2012), lyophilisation (Nie et al., 2012), gas foaming (Ji, Annabi, Hosseinkhani, Sivaloganathan, & Dehghani, 2012) and electrospinning (Tong & Wang, 2013). Freeze drying or lyophilisation is chosen as a suitable technique to work with aqueous suspension of polymer solutions, where the samples are initially frozen at low temperature and the frozen solvents are removed by sublimation under vacuum to obtain highly porous architecture (Liu, 2006).

The main challenges faced by pectin and CMC were poor mechanical strength and stiffness, whereas MFC contained short fibres (Qiu & Netravali, 2012). So, fabrication of lyophilised pectin/CMC/MFC composites is a potential way to address the application limitations of these polymers. Water soluble polymers like pectin and CMC were mixed to form interpolymer complexes with secondary bonds and MFC was incorporated to improve the mechanical performance of the scaffold.

The structural, thermal, mechanical and biological properties of the composite scaffolds are reported in this paper. The wound healing ability of these scaffolds on male Sprague-Dawley rats will be reported in the forthcoming paper.

2. Materials and methods

2.1. Materials

Pectin and CMC were purchased from Central Drug House Private Limited (Delhi, India). Glycerol (purity 99%) and anhydrous calcium chloride were bought from Sigma–Aldrich (Saint-Quentin Fallavier, France). Sodium hydroxide pellets were procured from Acros Organics (Illkirch Cedex, France). Vitacel® cellulose microfibers (MFC) were obtained from Rettenmair France SARL (Saint Germain En Laye, France). Phosphate buffered saline (PBS) powder, absolute ethanol, Dulbecco's Modified Eagle Medium (DMEM) and MTS reagent were acquired from Sigma–Aldrich. All the chemicals were used without any further purification. NIH 3T3 fibroblast cell lines were procured from ATCC cell biology collection.

2.2. Preparation of pectin/CMC/MFC porous scaffolds

A 2% (w/v) of pectin was prepared in distilled water by constant magnetic stirring. Simultaneously, 0.8% (w/v) of CMC was dissolved in water. Both these aqueous suspensions were then mixed well along with 4% (v/v) of glycerol and left for overnight stirring. Then, 0.1% (w/v) of MFC dispersed in distilled water was bath sonicated for 30 min and added to the mixture using syringe. The suspension was further crosslinked using 1% (w/v) calcium chloride (Fig. 1). The viscous suspension so obtained was poured onto petriplates and kept in deep freezer at −50 °C. These frozen samples were lyophilised in Christ Alpha 1–2 LD plus freeze dryer at −50 °C for 48 h to obtain porous scaffold, C(0.1%). Various samples were prepared by using 0%, 0.002%, 0.2% and 0.4% (w/v) of MFC, namely, C(0%), C(0.002%), C(0.2%) and C(0.4%), respectively.

2.3. Characterisation

The structural morphology of the fabricated scaffolds was investigated using scanning electron microscope (SEM) (JEOL, JSM 6031, Japan). Thin sections of the scaffolds were prepared using razor blade. They were sputtered with gold in vacuum using Polaron sputtering apparatus and the pore size was analysed. The three-dimensional (3D) images, porosity and pore size distribution of the prepared scaffolds were evaluated using micro computed tomography (m-CT) in Morlaix lab (France). The sample with thickness of 2.5 mm was scanned using monochromatic beam of X-rays directed from V (TOMEX) 240D X-ray tube operated at 240 kV and 320 W. It also had a precision manipulator whose length was 60 cm and maximum size of object diameter was 50 cm. The sample with voxel size of 4 μm was rotated through a full 360° and the two-dimensional (2D) X-ray images so obtained were reconstructed to obtain 3D images. The defect analysis was done to calculate the porosity. Fourier transform infrared spectra (FTIR) of the scaffolds were recorded using PerkinElmer spectrum D400, by scanning along a frequency ranging from 400 to 4000 cm^{-1}. X-ray diffraction (XRD) patterns of MFC powder and the synthesised scaffolds were obtained using Philips PW3710 diffractometer with Cu Kα radiation at a wavelength of 1.5418 Å. The diffraction spectra were verified over a 2θ range at room temperature with a scan rate of 0.018° s^{-1}. Thermogravimetric analysis (TGA) of the composite scaffolds and the neat polymers were carried out using Setaram DTA 92-10 thermal analyser using a scanning rate of 10 °C min^{-1} under nitrogen atmosphere, in a temperature range from 20 to 1000 °C. Differential scanning calorimetry (DSC) of the scaffolds was performed using Mettler-Toledo DSC-882 equipment. 10 mg of samples were heated from 10 to 40 °C at a heating rate of 10 °C min^{-1} in nitrogen atmosphere. The mechanical properties of the prepared scaffolds were determined using DMA 2980 TA instrument. The compression modulus and change in glass transition temperature were recorded by conducting a temperature sweep from 25 to 120 °C, at a heating rate of 10 °C/min. The samples were cut into rectangular shapes ($10 \times 10 \times 6\ mm^3$). The frequency was set at 1 Hz and displacement of 0.05 mm was used.

2.4. Water uptake studies

The water uptake ability of the scaffolds was analysed for 6 days. Small pieces of the scaffolds with equal weight (W_0) were immersed in deionised water, at room temperature. The wet weight of the samples (W) was determined after 2, 4 and 6 days, by gently blotting them on filter paper. The water uptake ability was calculated according to Eq. (2).

$$\text{water uptake ability}\,(\%) = \left[\frac{(W - W_0)}{W_0}\right] \times 100 \qquad (2)$$

2.5. In vitro degradation studies

In vitro biodegradation test of the scaffolds was performed by immersing equal weights (W_1) of samples in PBS (pH ~7.4) at 37 °C and incubated for 2, 4 and 6 days. The samples were removed after precised time duration, washed in deionised water and freeze dried. The final weight of the sample was noted (W_2). The percentage of

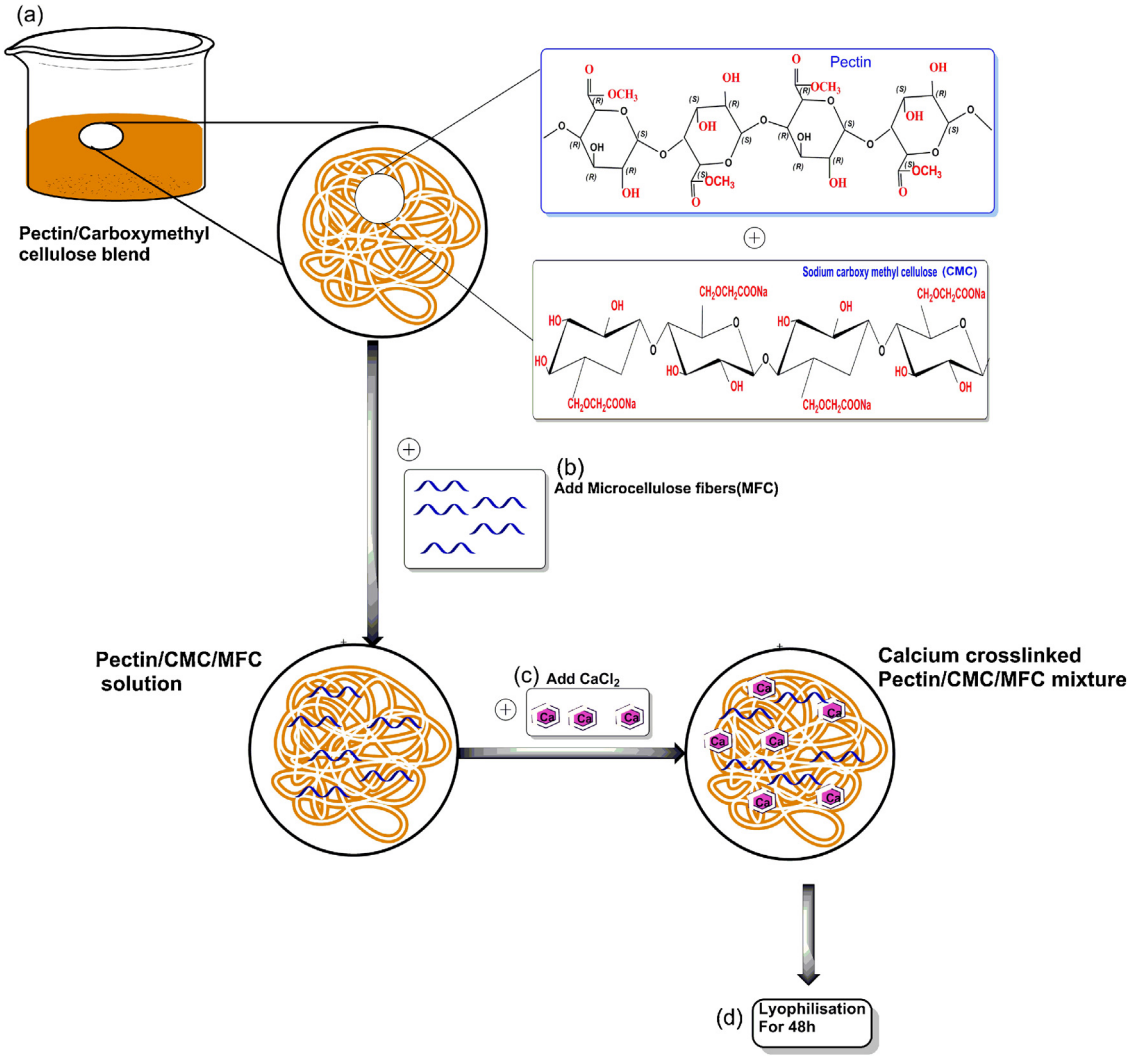

Fig. 1. Schematic representation of synthesis route of pectin/CMC/MFC composite scaffold.

degradation was calculated using Eq. (3) and recorded as mean ± SD ($n = 3$).

$$\text{degradation}\,(\%) = \left[\frac{(W_1 - W_2)}{W_1}\right] \times 100 \quad (3)$$

2.6. Cell viability studies

Cell viability of pectin/CMC (control) and pectin/CMC/MFC composite scaffolds was evaluated using MTS assay which is a colorimetric assay for determining the mitochondrial activity of viable cells that reduce the tetrazolium dye, MTS [3-(4,5-dimethylthiazol-2-yl)-5-(3-carboxy methoxy phenyl)-2-(4-sulfophenyl)-2H-tetrazolium] to purple coloured formazan product (Zhang, Wu, Friis, & Xiao, 2010). Triplicates of each sample were excised into pieces of equal weights and UV sterilised overnight. NIH 3T3 cells were harvested in DMEM medium and seeded onto 12 well plates at a density of 10^4 cells/ml and incubated at 37 °C. After the incubation period for 48 h, MTS solution was added and incubated further for 4 h, at 37 °C. The medium was transferred to 96-well plates and the absorbance was measured at 495 nm using microplate reader (Spectromax 180). Data were plotted as mean ± SD and cell viability was estimated.

3. Results and discussions

3.1. Structural analysis using SEM

The SEM images indicated the highly porous structure of prepared scaffold. The pore size was found in the range of 30–300 μm in case of C(0%) and 10–250 μm in case of C(0.1%). The slight decrease in pore size may be due to incorporation of filler (MFC), which impart good interaction with the polymers (Fig. 2). The pores aid in the migration, proliferation and differentiation of cells by providing better nutrient supply and vascularisation (Srinivasan, Jayasree, Chennazhi, Nair, & Jayakumar, 2012). The distribution of pores was more uniform when compared to C(0.1%). The surface of C(0.1%) was found to be smooth which further increased the bioactivity of scaffolds. Literature reported pore size in the range of 50–200 μm in case of pectin/poly(lactide-co-glycolide) scaffold (Liu et al., 2004); 10–50 μm for pectin/gelatin membrane (Mishra, Majeed, & Banthia, 2011); 100–200 μm for pectin/chitosan/nanohydroxyapatite composite (Li et al., 2011); and 50–300 μm for pectin/collagen scaffold (Sangsen, Benjakul, & Oungbho, 2011). Thus, the obtained pore size of synthesised pectin/CMC/MFC composite scaffolds is ideal for tissue engineering applications.

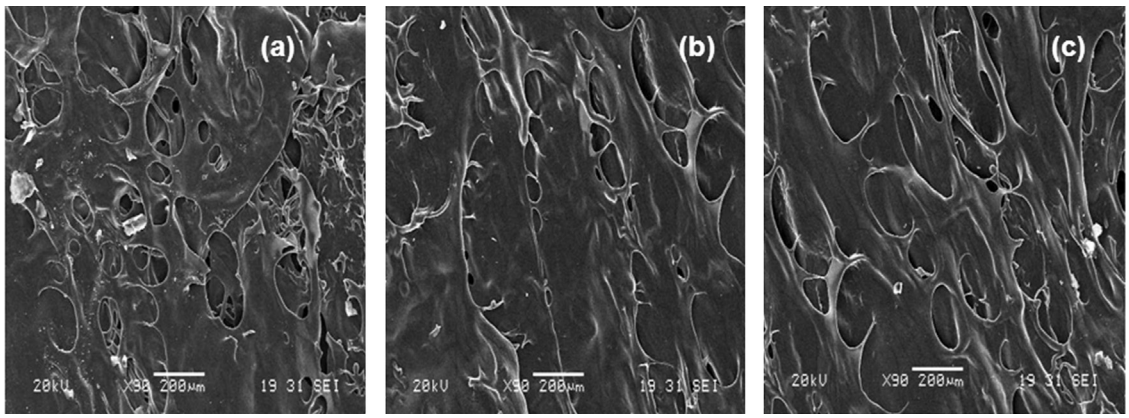

Fig. 2. SEM images showing macroporous structures of (a) C(0%); (b) C(0.1%).

3.2. Porosity estimation using micro-CT

Micro-CT was used to investigate the 3D porous architecture of pectin/CMC/MFC scaffold. Fig. 3(a) and (b) showed the side and cross sectional view of C(0.1%). These indicated that the pores were distributed throughout the scaffold. However, the pore size was found in the range of 15–280 μm. When compared to SEM, the pore size obtained in micro-CT analysis was comparatively higher because it was calculated based on the amount of pixels present in the pore (Dubruel et al., 2007). Majority of the pores (60%) were found to be less than 20 μm. Around 38% of pores were found in the range of 20–40 μm. Fig. 3(c) depicted the defect volume analysis of C(0.1%), in which porosity was estimated to be 88%. Porosity is a critical factor that determines factors like diffusion of nutrients and gases and proliferation of cells in case of tissue engineering scaffolds (Kane & Roeder, 2012).

3.3. Study of interaction among pectin, CMC and MFC using FTIR spectroscopy

The characteristic FTIR peaks of pectin were 3366 cm^{-1} due to —OH stretching vibration and 2931 cm^{-1} due to the stretching vibration of methyl group of methyl ester. The carbonyl absorption band at 1734 cm^{-1} was assigned to esterified carboxyl groups. The absorption bands at 1220 and 1008 cm^{-1} corresponded to ether (R–O–R) and C–C bond in the ring structure of pectin molecules. Weak symmetric carbonyl stretching vibrations were observed in the range of 800–1000 cm^{-1} (Coimbra et al., 2011; Monsoor, Kalapathy, & Proctor, 2001).

In the FTIR spectrum of CMC, the peak at 3367 cm^{-1} was due to —OH stretching vibrations. Symmetric and asymmetric modes of stretching vibration of carboxylic groups were observed at 1587 and 1416 cm^{-1}. Asymmetric stretching vibration modes of ether bonds were found in the range of 1020–1080 cm^{-1} (Bao, Ma, & Li, 2011; Luna-Martínez et al., 2011).

MFC showed characteristic absorption peaks of cellulose at 3334 cm^{-1} due to —OH stretching vibrations. Other peaks recorded were 2878 cm^{-1} due to —CH stretching vibrations, 1369 cm^{-1} for —CH bending vibrations, 1029 cm^{-1} for —CO stretching vibrations and 902 cm^{-1} for CH_2 stretching vibrations (Lu, Askeland, & Drzal, 2008).

FTIR spectra of pectin, CMC, MFC and C(0.1%) were compared in Fig. 4A. The variation in intensity and shifting of peaks from 3366 to 3271 cm^{-1}, in case of C(0.1%), were mainly attributed by the —OH stretching vibrations of CMC (Bao, Ma, & Li, 2011). The absorption bands of CMC and pectin, in the region from 1000 to 1200 cm^{-1} have become more prominent in case of C(0.1%), which showed the incorporation of MFC in the composite scaffold, that might have interacted with the ether groups of polymers through hydrogen bonds (Lu, Askeland, & Drzal, 2008). The bands associated with carboxylic groups of CMC and pectin, were shifted to higher wavenumber (1610 cm^{-1}) for C(0.1%), possibly due to crosslinking by Ca^{2+} ions (Luna-Martínez et al., 2011). Thus, the enhancement and shifts in the FTIR peaks could prove the favourable interactions of MFC with the polymers constituting the scaffold matrix. They could further confirm the crosslinking of polymers by calcium ions.

3.4. Crystallinity studies using XRD

Fig. 4B provided evidence of crystal morphology of the prepared scaffolds. The diffraction pattern of C(0%) displayed a broad peak at 21° showing low crystallinity of the polymer blends of pectin and CMC. MFC contains both crystalline and amorphous regions. The diffractogram of MFC showed three crystalline peaks at 16.19°, 22.5° (2θ) and 34°, respectively. The diffraction peak at 22.5° corresponds to (0 0 2) lattice plane (Sonia & Priya, 2013). The composites showed the characteristic peaks of MFC at 22.5° and 34°, whose intensity increased with increase in the concentration of filler. A direct relation was observed between intensity of diffraction peaks and concentration of MFC. These results confirmed the presence of crystalline MFC in the scaffold matrix.

3.5. Mechanical studies using DMA

The mechanical properties of porous scaffolds were analysed using DMA. In case of C(0%), the compression modulus was extremely low (~0.077 MPa). On the addition of MFC (filler), the compression modulus was found to increase and the optimum value was found to be 3.987 MPa, for C(0.1%) at 25 °C. On further addition of MFC, the modulus value dropped. DMA is the most appropriate method to investigate the relaxation events in polymeric scaffolds. Besides the modulus, tan δ can be calculated from the temperature sweep curve (Fig. 5). tan δ is the ratio of loss modulus to storage modulus. It is plotted against temperature and glass transition is found as a peak, as the scaffold material will absorb energy when it passes through the transition state (Menard, 2008). The glass transition temperature (T_g) was found to increase from 95 °C for C(0%) up to 116 °C for C(0.1%). On further addition of filler, T_g was found to decrease. The increase of T_g was ascribed to the favourable interactions between MFC and polymers, which partially hinder the chain mobility. On the other hand, the addition of MFC, beyond a particular concentration decreased the T_g

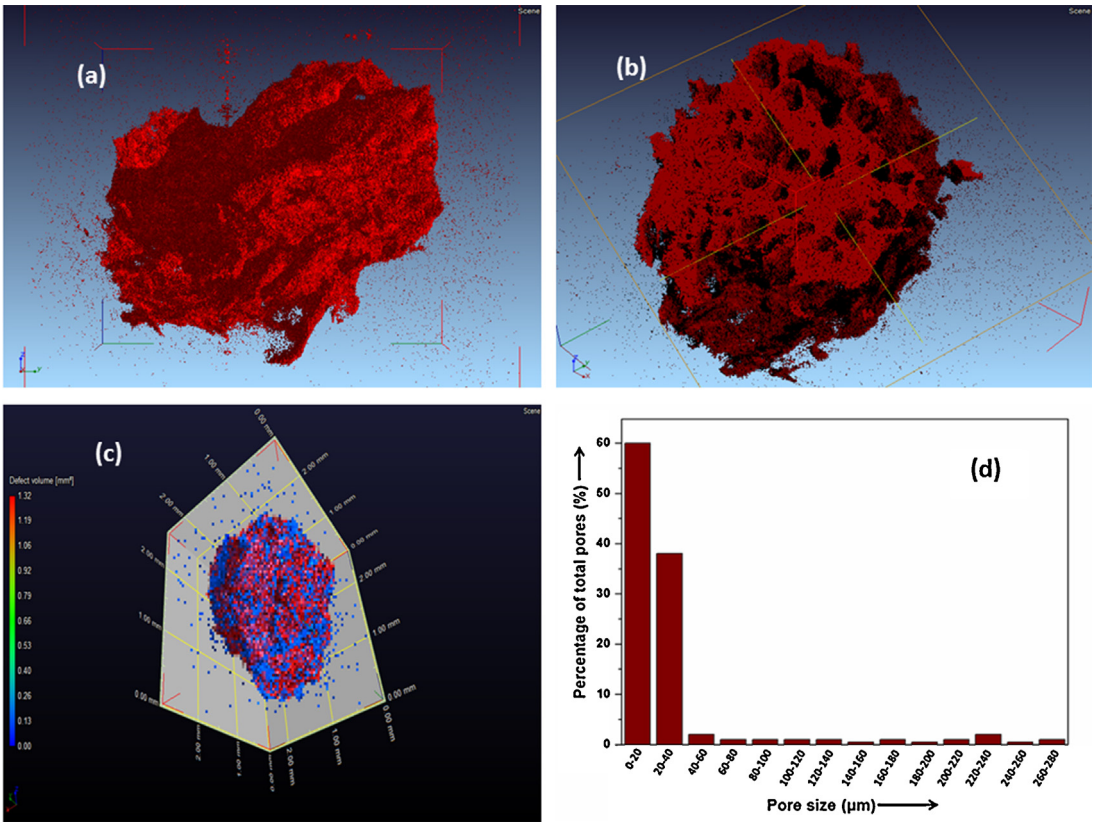

Fig. 3. Micro-CT images: (a) side view, (b) cross-sectional view of (c) defect volume analysis for estimation of porosity. (d) Pore size distribution of C(0.1%).

by increasing the mobility of some polymer segments after freezing the more rigid ones onto the MFC surface. This was consistent with the T_g measurements in the following paragraph. C(0.1%) was found to have the highest compression modulus and T_g, due to good dispersion of MFC in the hydrophilic matrix, held by hydrogen bonds. Previous reports have stated that MFC act as excellent fillers to improve the mechanical properties of composites (Xing et al., 2010). Our studies further confirmed the efficiency of MFC as excellent fillers.

3.6. Thermal analysis using DSC

Fig. 6 showed the DSC thermograms of the prepared scaffolds. T_g was observed at 82 °C for C(0%). On the addition of MFC, the T_g was found to increase up to 103° for C(0.1%). At higher concentrations of MFC, T_g dropped further, as observed by DMA, due to large surface availability for rigid segment adsorption. C(0.1%) has the highest T_g due to good interaction between polymer and filler. Droste and co-worker reported that interaction between filler particles and

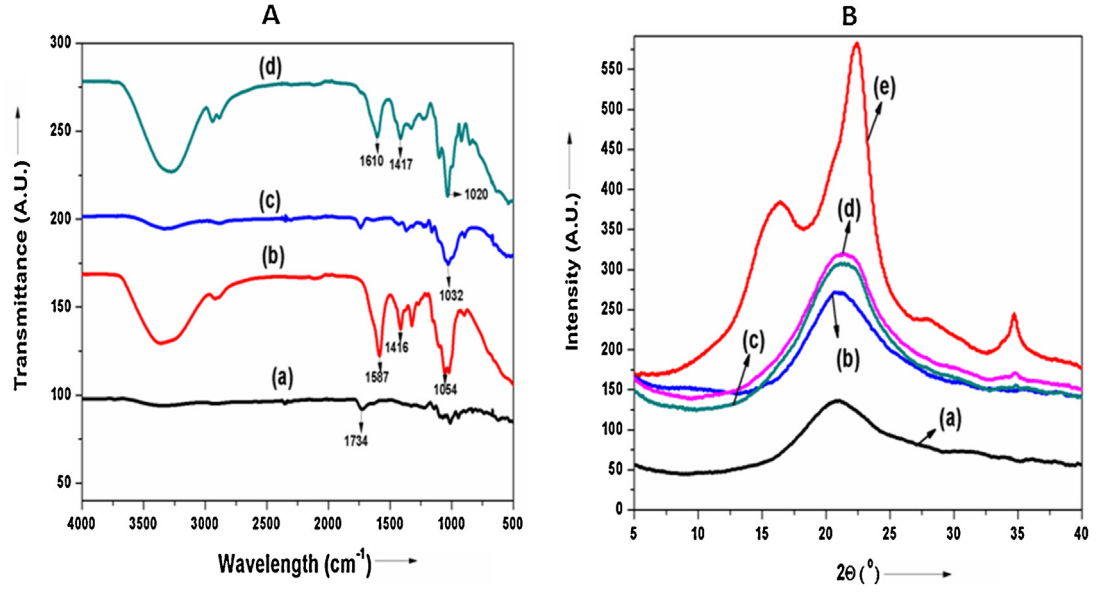

Fig. 4. (A) FTIR spectra of (a) pectin, (b) CMC, (c) MFC and (d) C(0.1%). (B) XRD spectra of (a) C(0%), (b) C(0.1%), (c) C(0.2%), (d) C(0.4%) and (e) MFC.

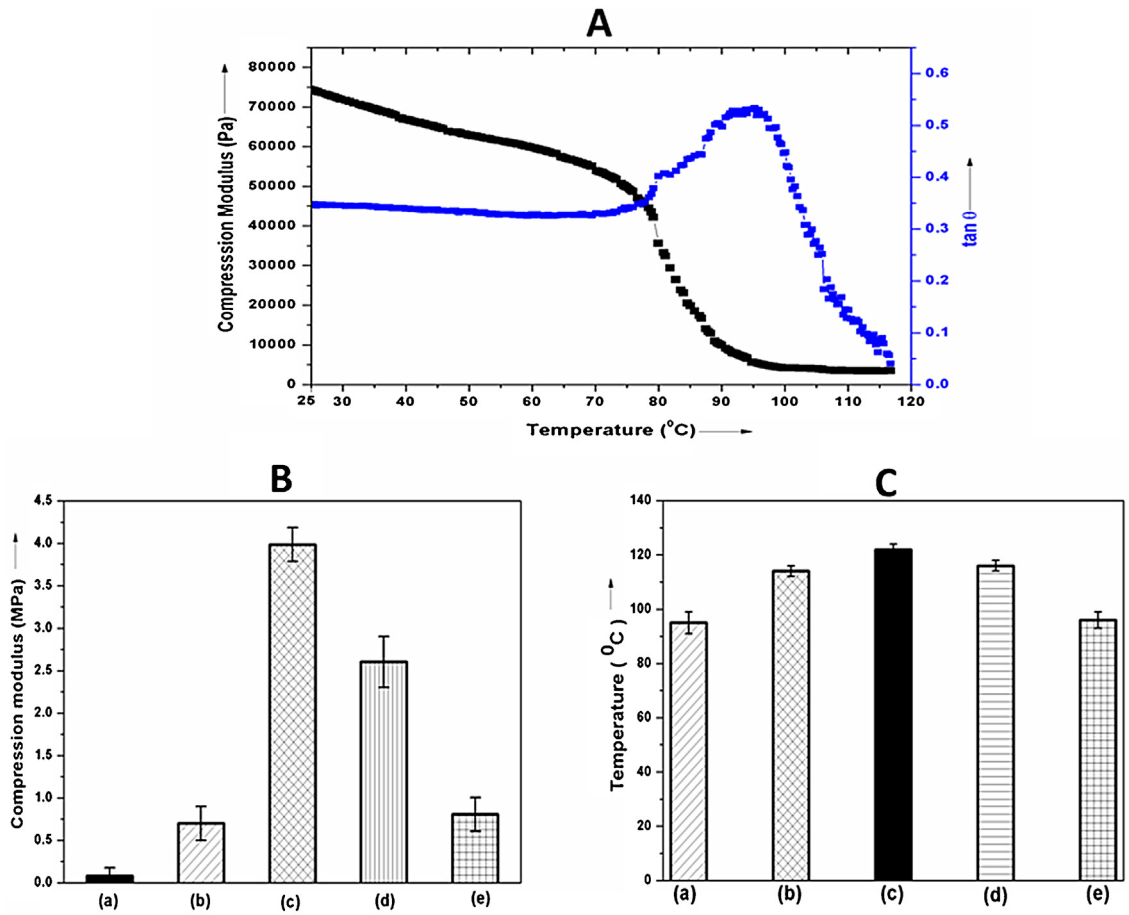

Fig. 5. (A) DMA temperature sweep curve of C(0.1%) at constant frequency of 1 Hz. Variation of (B) compression modulus and (C) glass transition temperature in case of (a) C(0%), (b) C(0.002%), (c) C(0.1%), (d) C(0.2%) and (e) C(0.4%).

polymers reduced the molecular mobility and flexibility of polymer chains and thus higher temperature was required for transition from glassy state to rubbery state (Droste & Dibenedetto, 1969). The results obtained from DSC were in agreement with DMA, but the values varied by a small factor.

3.7. Thermogravimetric (TGA) and differential thermal analysis (DTA)

Fig. 7 depicted the TGA profile which showed a first decomposition in the range of 30–95 °C for C(0%) and 100–160 °C for C(0%), due to loss of moisture. A second decomposition was found in the range of 160–275 °C for C(0%) and 265–390 °C for C(0.1%). These data proved that C(0.1%) showed better thermal stability than C(0%), due to excellent reinforcement of MFC in the matrix.

The DTA curve implied that C(0.1%) exhibited slow degradation rate compared to C(0%). This may be due to incorporation of MFC in the polymer scaffold and their effective reinforcement within the matrix. The endothermic peak observed at 240 °C can be due to decomposition of polysaccharides constituting the scaffold (Bhatt, Gupta, & Naithani, 2011; Nada & Hassan, 2000).

3.8. Water uptake studies

The water uptake ability of C(0%) and composite scaffolds were shown in Fig. 8A. Among the different test samples, C(0.1%) showed lowest swelling. This is attributed due to good interaction between polymers and incorporated organic fillers. On the second day, C(0%) showed 78% uptake of water while C(0.1%) showed 63% uptake. The rate of water uptake was found to upsurge with increase in time. On the sixth day, the percentage of water uptake was 96 and 85%, in case of C(0%) and C(0.1%), respectively. All the scaffolds attained maximum swelling capacity and thereafter they started degrading due to rupture of polymer chains (Erol et al., 2012). The parameters like swelling and porosity of scaffolds help in the uptake of nutrients to the interior of porous scaffolds.

3.9. In vitro degradation studies

The *in vitro* degradation profiles of pectin/CMC and pectin/CMC/MFC composite scaffolds were shown in Fig. 8B. The rate of degradation of C(0.1%) was slightly less compared to C(0%) due to better interaction between the polymers and the filler. On second day, C(0.1%) underwent 34% degradation while 51% degradation was observed in case of C(0%). On sixth day, 65% of C(0.1%) underwent degradation whereas nearly 81% of C(0%) got degraded. These studies further support that there was good interaction between polymers and fillers, in case of C(0.1%),which aided in reduced degradation. The possible reason for scaffold degradation is the displacement of calcium ions that crosslink the scaffold matrix by sodium, potassium and phosphate ions in the PBS along with preferential dissolution of hydrophilic polymers (Hunt, Smith, Gbureck, Shelton, & Grover, 2010). As time increased, degradation rates of scaffolds were found to increase. Among the different porous scaffolds, C(0.1%) showed minimum and controlled degradation rate.

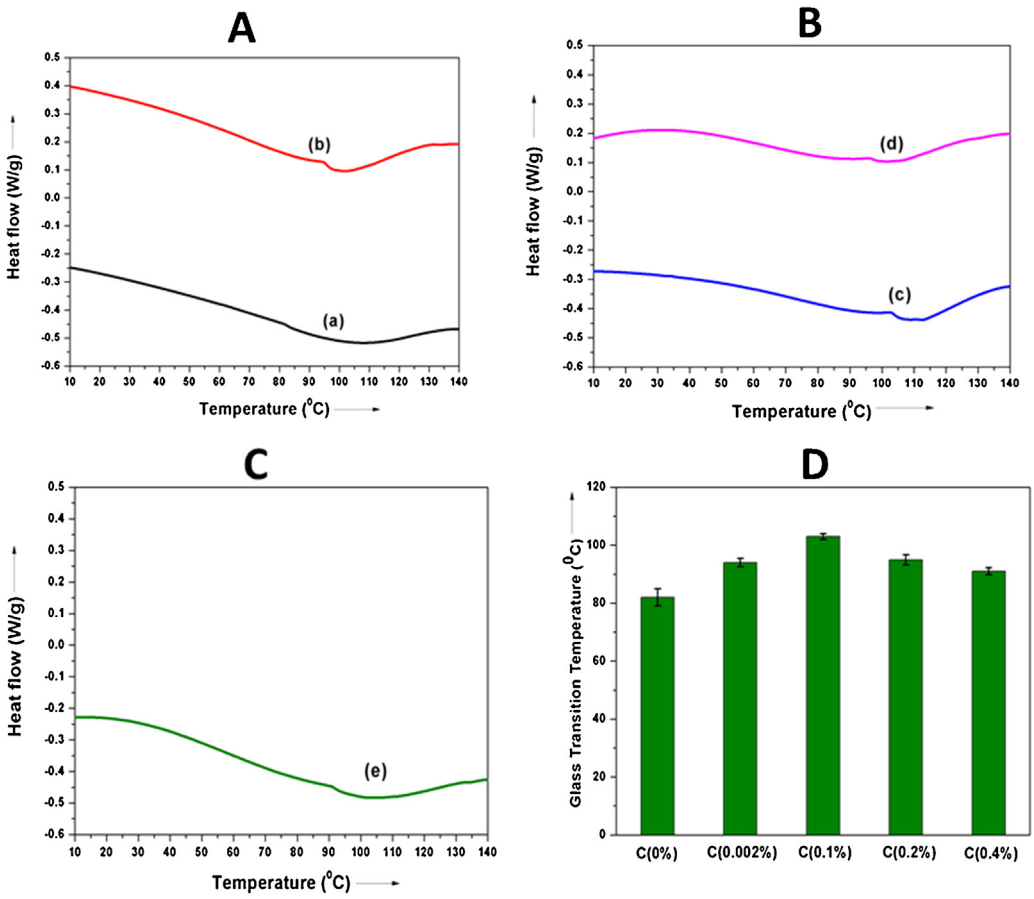

Fig. 6. DSC thermograms (A) of (a) C(0%) and (b) C(0.002%); (B) of C(0.1%) and C(0.2%); (C) of (e) C(0.4%). (D) Variation of glass transition temperature.

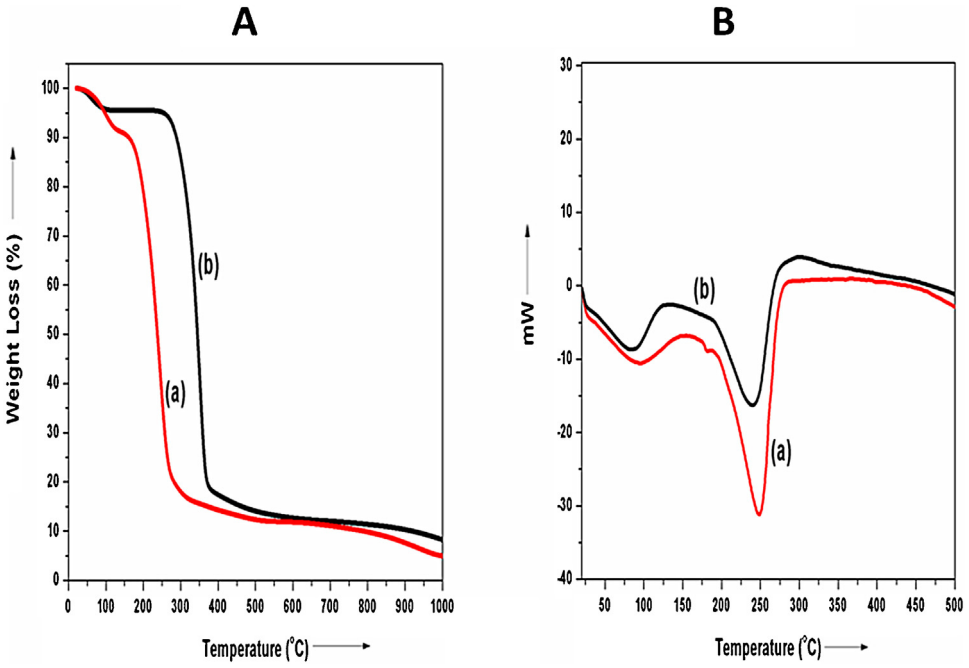

Fig. 7. (A) TGA and (B) DTA profiles of (a) C(0%) and (b) C(0.1%).

3.10. Cell viability studies

Cytocompatibility of pectin/CMC (control) and pectin/CMC/MFC composite scaffolds were assessed using MTS assay using NIH3T3 cells. Among the tested samples, C(0.1%) showed the highest cytocompatibility after 48 h (Fig. 8C). The possible reason for apoptosis of cells in case of all other composites was the chance of leaching due to poor interaction between the polymers and filler, leading

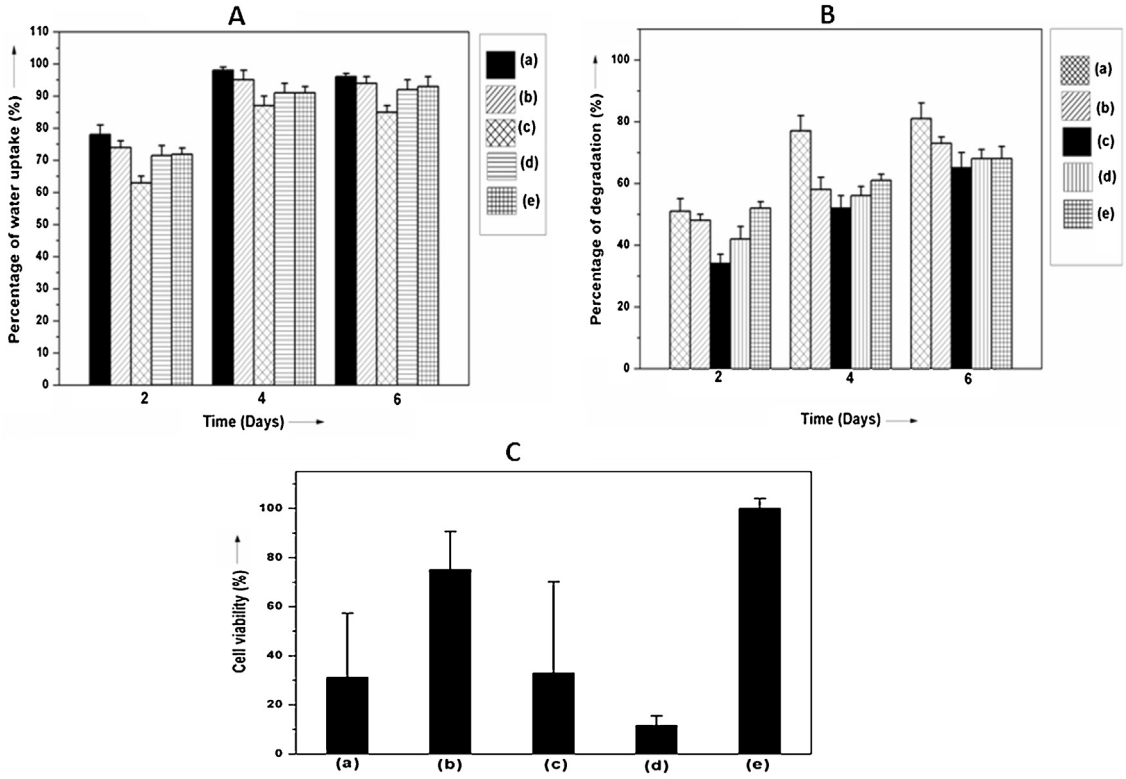

Fig. 8. (A) Water uptake ability and (B) *in vitro* degradation studies of (a) C(0%), (b) C(0.002%), (c) C(0.1%), (d) C(0.2%) and (e) C(0.4%). (C) Cell viability of (a) C(0%), (b) C(0.1%), (c) C(0.2%), (d) C(0.4%) and (e) control cells.

to influx of Ca^{2+} ions in the culture medium (Lang & Hoffmann, 2012). Compared to the positive control cells, there was no significant reduction in cell viability of C(0.1%), stating that the composite scaffolds were biocompatible.

4. Conclusion

Pectin/CMC/MFC scaffolds were successfully fabricated using lyophilisation technique. The composite scaffolds with 0.1% MFC [C(0.1%)], had pore size in the range of 10–250 μm, which were ideal for tissue engineering applications. The porosity of C(0.1%) was estimated to be 88% which enabled diffusion of nutrients and cell proliferation. The FTIR peaks could confirm the incorporation of MFC within the polymer matrix and crosslinking of scaffolds by calcium ions. XRD diffractogram further confirmed the presence of MFC by exhibiting its crystalline lattice planes in composite scaffolds. C(0.1%) showed highest compression modulus (~3.987 MPa) and T_g (~103°). The DSC results were in agreement with DMA results in case of variation of T_g with concentration of fillers. C(0.1%) showed excellent thermal stability and low degradation rate compared to C(0%). It also demonstrated controlled swelling and degradation and highest cell viability among the various composite scaffolds. All these results suggested that pectin/CMC/MFC scaffolds can prove to be ideal polymeric matrix for tissue regeneration.

Acknowledgements

We acknowledge financial support rendered by Brittany region, The European Union (FEDER) and the French Ministry for research for conducting the studies.

References

Agoda-Tandjawa, G., Durand, S., Gaillard, C., Garnier, C., & Doublier, J. L. (2012). Rheological behaviour and microstructure of microfibrillated cellulose suspensions/low-methoxyl pectin mixed systems. Effect of calcium ions. *Carbohydrate Polymers*, *87*(2), 1045–1057.

Bao, Y., Ma, J., & Li, N. (2011). Synthesis and swelling behaviors of sodium carboxymethyl cellulose-g-poly(AA-co-AM-co-AMPS)/MMT superabsorbent hydrogel. *Carbohydrate Polymers*, *84*(1), 76–82.

Bhatt, N., Gupta, P. K., & Naithani, S. (2011). Hydroxypropyl cellulose from α-cellulose isolated from *Lantana camara* with respect to DS and rheological behavior. *Carbohydrate Polymers*, *86*(4), 1519–1524.

Chen, H., & Fan, M. (2007). Chitosan/carboxymethyl cellulose polyelectrolyte complex scaffolds for pulp cells regeneration. *Journal of Bioactive and Compatible Polymers*, *22*(5), 475–491.

Coimbra, P., Ferreira, P., de Sousa, H. C., Batista, P., Rodrigues, M. A., Correia, I. J., et al. (2011). Preparation and chemical and biological characterization of a pectin/chitosan polyelectrolyte complex scaffold for possible bone tissue engineering applications. *International Journal of Biological Macromolecules*, *48*(1), 112–118.

Di Spiezio Sardo, A., Spinelli, M., Bramante, S., Scognamiglio, M., Greco, E., Guida, M., et al. (2011). Efficacy of a polyethylene oxide-sodium carboxymethyl cellulose gel in prevention of intrauterine adhesions after hysteroscopic surgery. *Journal of Minimally Invasive Gynecology*, *18*(4), 462–469.

Droste, D. H., & Dibenedetto, A. T. (1969). The glass transition temperature of filled polymers and its effect on their physical properties. *Journal of Applied Polymer Science*, *13*, 2149–2168.

Dubruel, P., Unger, R., Van Vlierberghe, S., Cnudde, V., Jacobs, P. J. S., Schacht, E., et al. (2007). Porous gelatin hydrogels: 2. In vitro cell interaction study. *Biomacromolecules*, *8*, 338–344.

Dutta, R. K., & Sahu, S. (2012). Development of oxaliplatin encapsulated in magnetic nanocarriers of pectin as a potential targeted drug delivery for cancer therapy. *Results in Pharma Sciences*, *2*, 38–45.

Erol, M. M., Mouriño, V., Newby, P., Chatzistavrou, X., Roether, J. A., Hupa, L., et al. (2012). Copper-releasing, boron-containing bioactive glass-based scaffolds coated with alginate for bone tissue engineering. *Acta Biomaterialia*, *8*(2), 792–801.

García-González, C. A., Alnaief, M., & Smirnova, I. (2011). Polysaccharide-based aerogels—promising biodegradable carriers for drug delivery systems. *Carbohydrate Polymers*, *86*(4), 1425–1438.

Ghanbarzadeh, B., & Almasi, H. (2011). Physical properties of edible emulsified films based on carboxymethyl cellulose and oleic acid. *International Journal of Biological Macromolecules*, *48*(1), 44–49.

Hunt, N. C., Smith, A. M., Gbureck, U., Shelton, R. M., & Grover, L. M. (2010). Encapsulation of fibroblasts causes accelerated alginate hydrogel degradation. *Acta Biomaterialia*, *6*(9), 3649–3656.
Ji, C., Annabi, N., Hosseinkhani, M., Sivaloganathan, S., & Dehghani, F. (2012). Fabrication of poly-DL-lactide/polyethylene glycol scaffolds using the gas foaming technique. *Acta Biomaterialia*, *8*(2), 570–578.
Kane, R. J., & Roeder, R. K. (2012). Effects of hydroxyapatite reinforcement on the architecture and mechanical properties of freeze-dried collagen scaffolds. *Journal of the Mechanical Behavior of Biomedical Materials*, *7*, 41–49.
Katav, T., Liu, L., Traitel, T., Goldbart, R., Wolfson, M., & Kost, J. (2008). Modified pectin-based carrier for gene delivery: Cellular barriers in gene delivery course. *Journal of Controlled Release*, *130*(2), 183–191.
Khanarian, N. T., Haney, N. M., Burga, R. A., & Lu, H. H. (2012). A functional agarose-hydroxyapatite scaffold for osteochondral interface regeneration. *Biomaterials*, *33*(21), 5247–5258.
Lang, F., & Hoffmann, E. K. (2012). Role of ion transport in control of apoptotic cell death. *Comprehensive Physiology*, *2*, 2037–2061.
Lavoine, N., Desloges, I., Dufresne, A., & Bras, J. (2012). Microfibrillated cellulose – its barrier properties and applications in cellulosic materials: A review. *Carbohydrate Polymers*, *90*(2), 735–764.
Lee, F., & Kurisawa, M. (2013). Formation and stability of interpenetrating polymer network hydrogels consisting of fibrin and hyaluronic acid for tissue engineering. *Acta Biomaterialia*, *9*(2), 5143–5152.
Li, J., Sun, H., Sun, D., Yao, Y., Yao, F., & Yao, K. (2011). Biomimetic multicomponent polysaccharide/nano-hydroxyapatite composites for bone tissue engineering. *Carbohydrate Polymers*, *85*(4), 885–894.
Liu, J. (2006). Physical characterization of pharmaceutical formulations in frozen and freeze dried solid states: Techniques and applications in freeze drying development. *Pharmaceutical Development and Technology*, *11*, 3–28.
Lönnberg, H., Fogelström, L., Berglund, L., Malmström, E., & Hult, A. (2008). Surface grafting of microfibrillated cellulose with poly(ε-caprolactone)—synthesis and characterization. *European Polymer Journal*, *44*(9), 2991–2997.
Liu, L., Won, Y. J., Cooke, P. H., Coffin, D. R., Fishman, M. L., Hicks, K. B., et al. (2004). Pectin/poly(lactide-co-glycolide) composite matrices for biomedical applications. *Biomaterials*, *25*, 3201–3210.
Lu, J., Askeland, P., & Drzal, L. T. (2008). Surface modification of microfibrillated cellulose for epoxy composite applications. *Polymer*, *49*(5), 1285–1296.
Luna-Martínez, J. F., Hernández-Uresti, D. B., Reyes-Melo, M. E., Guerrero-Salazar, C. A., González-González, V. A., & Sepúlveda-Guzmán, S. (2011). Synthesis and optical characterization of ZnS–sodium carboxymethyl cellulose nanocomposite films. *Carbohydrate Polymers*, *84*(1), 566–570.
Malafaya, P. B., Silva, G. A., & Reis, R. L. (2007). Natural-origin polymers as carriers and scaffolds for biomolecules and cell delivery in tissue engineering applications. *Advanced Drug Delivery Reviews*, *59*, 207–233.
Menard, K. P. (2008). *Dynamic mechanical analysis: A practical introduction* (2nd ed.). CRC: Taylor & Francis (Chapter 1).
Mishra, R. K., Majeed, A. B. A., & Banthia, A. K. (2011). Development and characterization of pectin/gelatin hydrogel membranes for wound dressing. *International Journal of Plastics Technology*, *15*(1), 82–95.
Monsoor, M. A., Kalapathy, U., & Proctor, A. (2001). Determination of polygalacturonic acid content in pectin extracts by diffuse reflectance Fourier transform infrared spectroscopy. *Food Chemistry*, *74*(2), 233–238.
Munarin, F., Guerreiro, S. G., Grellier, M. A., Tanzi, M. C., Barbosa, M. A., Petrini, P., et al. (2011). Pectin-based injectable biomaterials for bone tissue engineering. *Biomacromolecules*, *12*(3), 568–577.
Munarin, F., Tanzi, M. C., & Petrini, P. (2012). Advances in biomedical applications of pectin gels. *International Journal of Biological Macromolecules*, *51*(4), 681–689.
Nada, A. M. A., & Hassan, M. L. (2000). Thermal behavior of cellulose and some cellulose derivatives. *Polymer Degradation and Stability*, *67*(1), 111–115.
Nie, L., Chen, D., Suo, J., Zou, P., Feng, S., Yang, Q., et al. (2012). Physicochemical characterization and biocompatibility in vitro of biphasic calcium phosphate/polyvinyl alcohol scaffolds prepared by freeze-drying method for bone tissue engineering applications. *Colloids and Surfaces B: Biointerfaces*, *100*(1), 169–176.
Nunes, C., Silva, L., Fernandes, A. P., Guiné, R. P. F., Domingues, M. R. M., & Coimbra, M. A. (2012). Occurrence of cellobiose residues directly linked to galacturonic acid in pectic polysaccharides. *Carbohydrate Polymers*, *87*(1), 620–626.
Pooyan, P., Tannenbaum, R., & Garmestani, H. (2012). Mechanical behavior of a cellulose-reinforced scaffold in vascular tissue engineering. *Journal of the Mechanical Behavior of Biomedical Materials*, *7*, 50–59.
Qiu, K., & Netravali, A. N. (2012). Fabrication and characterization of biodegradable composites based on microfibrillated cellulose and polyvinyl alcohol. *Composites Science and Technology*, *72*(13), 1588–1594.
Ramli, N. A., & Wong, T. W. (2011). Sodium carboxymethylcellulose scaffolds and their physicochemical effects on partial thickness wound healing. *International Journal of Pharmaceutics*, *403*(1–2), 73–82.
Rodrigues, A. I., Gomes, M. E., Leonor, I. B., & Reis, R. L. (2012). Bioactive starch-based scaffolds and human adipose stem cells are a good combination for bone tissue engineering. *Acta Biomaterialia*, *8*(10), 3765–3776.
Sangsen, Y., Benjakul, S., & Oungbho, K. (2011). Fabrication of novel shark collagen-pectin scaffolds for tissue engineering. In *Biomedical Engineering International Conference (BMEiCON)* (pp. 273–278).
Shachar, M., Tsur-Gang, O., Dvir, T., Leor, J., & Cohen, S. (2011). The effect of immobilized RGD peptide in alginate scaffolds on cardiac tissue engineering. *Acta Biomaterialia*, *7*(1), 152–162.
Shao, J., Chen, C., Wang, Y., Chen, X., & Du, C. (2012). Early stage structural evolution of PLLA porous scaffolds in thermally induced phase separation process and the corresponding biodegradability and biological property. *Polymer Degradation and Stability*, *97*(6), 955–963.
Sin, D., Miao, X., Liu, G., Wei, F., Chadwick, G., Yan, C., et al. (2010). Polyurethane (PU) scaffolds prepared by solvent casting/particulate leaching (SCPL) combined with centrifugation. *Materials Science and Engineering C*, *30*(1), 78–85.
Sionkowska, A., & Płanecka, A. (2013). Preparation and characterization of silk fibroin/chitosan composite sponges for tissue engineering. *Journal of Molecular Liquids*, *178*, 5–14.
Smistad, G., Bøyum, S., Alund, S. J., Samuelsen, A. B. C., & Hiorth, M. (2012). The potential of pectin as a stabilizer for liposomal drug delivery systems. *Carbohydrate Polymers*, *90*(3), 1337–1344.
Sonia, A., & Priya, D. K. (2013). Chemical, morphology and thermal evaluation of cellulose microfibers obtained from *Hibiscus sabdariffa*. *Carbohydrate Polymers*, *92*(1), 668–674.
Srinivasan, S., Jayasree, R., Chennazhi, K. P., Nair, S. V., & Jayakumar, R. (2012). Biocompatible alginate/nano bioactive glass ceramic composite scaffolds for periodontal tissue regeneration. *Carbohydrate Polymers*, *87*, 274–283.
Sudheesh Kumar, P. T., Srinivasan, S., Lakshmanan, V.-K., Tamura, H., Nair, S. V., & Jayakumar, R. (2011). β-Chitin hydrogel/nano hydroxyapatite composite scaffolds for tissue engineering applications. *Carbohydrate Polymers*, *85*(3), 584–591.
Suryanegara, L., Nakagaito, A. N., & Yano, H. (2009). The effect of crystallization of PLA on the thermal and mechanical properties of microfibrillated cellulose-reinforced PLA composites. *Composites Science and Technology*, *69*(7–8), 1187–1192.
Tong, H.-W., & Wang, M. (2013). A novel technique for the fabrication of 3D nanofibrous scaffolds using simultaneous positive voltage electrospinning and negative voltage electrospinning. *Materials Letters*, *94*(1), 116–120.
Tripathy, J., & Raichur, A. M. (2013). Designing carboxymethyl cellulose based layer-by-layer capsules as a carrier for protein delivery. *Colloids and Surfaces B: Biointerfaces*, *101*, 487–492.
Van Vlierberghe, S., Dubruel, P., & Schacht, E. (2011). Biopolymer-based hydrogels as scaffolds for tissue engineering applications: A review. *Biomacromolecules*, *12*(5), 1387–1408.
Wan, Y. Z., Luo, H., He, F., Liang, H., Huang, Y., & Li, X. L. (2009). Mechanical, moisture absorption, and biodegradation behaviours of bacterial cellulose fibre-reinforced starch biocomposites. *Composites Science and Technology*, *69*(7–8), 1212–1217.
Wang, W., & Wang, A. (2010). Nanocomposite of carboxymethyl cellulose and attapulgite as a novel pH-sensitive superabsorbent: Synthesis, characterization and properties. *Carbohydrate Polymers*, *82*, 83–91.
Xing, Q., Zhao, F., Chen, S., McNamara, J., DeCoster, M. A., & Lvov, Y. M. (2010). Porous biocompatible three-dimensional scaffolds of cellulose microfiber/gelatin composites for cell culture. *Acta Biomaterialia*, *6*(6), 2132–2139.
Zhang, Y., Wu, C., Friis, T., & Xiao, Y. (2010). The osteogenic properties of CaP/silk composite scaffolds. *Biomaterials*, *31*(10), 2848–2856.